Stability analysis of parked wind turbine blades

E. S. Politis and P. K. Chaviaropoulos
Centre for Renewable Energy Sources
19th km Marathonos Av., 19009, Pikermi, Greece
vpolitis@cres.gr, tchaviar@cres.gr

V. A. Riziotis and S. G. Voutsinas
National Technical University of Athens
9 Heroon Polytechniou str., 15780, Athens, Greece
vasilis@fluid.mech.ntua.gr, spyros@fluid.mech.ntua.gr

I. Romero-Sanz
Technology Department, Gamesa
Ramírez de Arellano 37, 28043 Madrid, Spain
iromero@gamesacorp.com

Abstract

Wind turbine blades in parked position can experience extremely high flow angles of attack in the region of ±90°, depending on the direction of the incoming wind. Under such conditions the flow is massively separated over the entire blade span and therefore stall induced vibrations are likely to occur with obvious implications on loads and stability. The present paper focuses on the stability problem. The linear stability tool of CRES and NTUA is employed with the aim to investigate the aeroelastic stability of isolated parked blades for winds coming from all possible directions with respect to the rotor plane and wind speeds ranging from the cut in up to the survival speed. Results are presented for a reference blade (around 40 m) designed in the framework of the EU project UPWIND, under the Work Package 1B1 led by GAMESA. The results obtained indicate that more severe stall induced vibrations take place when the incoming wind direction is such that the local to the blade angles of attack are either around ±90° or close to the maximum C_L value.

Keywords: aeroelastic stability, parked conditions, wind turbine blades

1 Introduction

The blades of a parked wind turbine are usually exposed to local flow angles of attack in the vicinity of ±90°. At such extreme angles of attack massive flow separation occurs over the whole blade span and hence stall induced vibrations are very likely to follow. Such vibrations might generate load variations that can substantially contribute to the fatigue of the machine. Also, in conjunction with extreme winds of 50 years recurrence, they can result in critical loading situations that drive design loads.

The problem of stall induced instabilities has been given a lot of attention by the wind energy community during the last 15 years. Big effort has been put in the investigation of the edgewise vibrations occurring on stall regulated rotor blades when operating at high wind speeds, beyond rated conditions [1],[2],[3],[4]. This effort was combined with the in parallel development and implementation of various engineering dynamic stall models into the state of the art aeroelastic tools [3],[5],[6]. Moreover, substantial understanding of the underlying physical mechanisms was also provided through the use of CFD analysis in investigating dynamic stall phenomenon [7],[8],[9]. Of course all the above developments focused on instability problems occurring under normal operation, which inevitably limits angles of attack to values slightly above C_{Lmax} angles. Recently the problem of stall induced instabilities, occurring on parked rotors, has been introduced as one of the topics that need to be dealt with in the near feature [10]. However, until today very limited work has been reported on this topic [11], at least to the knowledge of the authors.

The greatest uncertainty in the aeroelastic modelling of a standing still wind turbine is the prediction of the aerodynamic loads of the fully separated flow over the blades. All existing engineering dynamic stall models provide aerodynamic loads in deep stall conditions for angles of attack lying in the region of the

maximum lift (C_{Lmax}) angle. However, none of them is properly tuned or validated in cases where the local flow incidence reaches 90^o. On the other hand, calculation of the wake induced effects of the non-rotating blade requires a different treatment than that offered in the context of the actuator disk theory. Despite the above uncertainties, the wind turbine standards require that manufacturers are able to demonstrate that their parked wind turbines can withstand the loads resulting from high winds coming from all possible directions (including extreme yaw misalignments of $\pm 180^o$). The above requirement, in combination with the uncertainties associated with determining loads in deep stall flows, emerges a substantial gap in the prediction capabilities of modern aeroelastic, even state-of-the-art, tools.

In the present paper, the aeroelastic stability of a parked wind turbine rotor is addressed. The work has been carried out in the framework of the EU funded project UPWIND, under Work Package 1B1. The analysis is performed for a paper case blade (around 40 m) of a 2MW pitch regulated–variable speed wind turbine, specifically designed for the purposes of the project.

As a starting point for the evaluation of the performance of the parked blade, its stability during operation is presented for uniform inflow. Then, the stability of the parked blade is considered in the context of the linear eigenvalue analysis, assuming steady state aerodynamics (unsteady vortex shedding is not taken into account). Stability computations are performed for an isolated, parked blade, for wind speeds up to the survival speed of 70 m/s and for yaw error angles ranging from -180^0 to $+180^0$. As already mentioned, the use of steady state aerodynamics in predicting highly separated flows corresponds to the prediction status of all existing state-of-the-art aeroelastic design tools employed in the certification of modern wind turbines.

Given the difficulties described above, associated with the prediction of the aerodynamic loads in deep stall conditions, the analysis is aimed at providing some first estimate of the incoming flow angle regimes for which stall induced vibrations become more pronounced. The results of the steady state analysis are also compared against stability predictions obtained using the unsteady aerodynamic model ONERA. This comparison is only applicable at relatively low yaw error angles where local flow angles of attack remain moderate and therefore ONERA model predictions are still valid.

2 The Stability Tool

Stability computations are performed by solving the eigenvalue problem of the linearized system of the coupled structural dynamic and aerodynamic equations of motion. The model is capable of treating the complete wind turbine configuration including the controls (servo-aeroelastic system) [12], [13]. In the baseline aeroelastic tool, structural dynamics are modelled using beam theory for all flexible components (i.e. the blades, the shaft and the tower) undergoing bending in two directions, torsion and tension. The approximation is based on the finite element method which results in beam elements of twelve degrees of freedom (DOFs). The dynamic and structural coupling of the different components is performed in the context of a multi-body analysis. Therefore in addition to their structural deformations, each deformable component is allowed to undergo rigid body motions under kinematic and load constraints specified by its connection to the remaining structure [14].

Rotor aerodynamics is modelled using blade element momentum theory employing quasi-steady or unsteady aerodynamic modelling (including dynamic stall modelling). In the first case, the 2D steady-state polars of the airfoils are introduced. On the other hand, localised unsteady aerodynamics is accounted for by the Extended ONERA Lift, Drag and Moment model [15]. Blade element momentum theory was devised for operating rotors. In parked conditions, wake effects are neglected and 2D strip theory is applied.

For the combined treatment of the aerodynamics and the structural dynamics, additional, aerodynamic states, corresponding to the circulation DOFs of the ONERA model, are introduced. They are combined with the structural ones in the so-called 'Aeroelastic Beam Element' [3].

The linearized system of the coupled aeroelastic equations of motion is written in the following form:

$$\begin{bmatrix} \boldsymbol{m}_{uu} & \boldsymbol{m}_{uq} \\ \boldsymbol{m}_{qu} & \boldsymbol{m}_{qq} \end{bmatrix} \cdot \begin{Bmatrix} \ddot{\boldsymbol{u}} \\ \ddot{\boldsymbol{q}} \end{Bmatrix} + \begin{bmatrix} \boldsymbol{d}_{uu} & \boldsymbol{d}_{uq} \\ \boldsymbol{d}_{qu} & \boldsymbol{d}_{qq} \end{bmatrix} \cdot \begin{Bmatrix} \dot{\boldsymbol{u}} \\ \dot{\boldsymbol{q}} \end{Bmatrix} + \begin{bmatrix} \boldsymbol{c}_{uu} & \boldsymbol{c}_{uq} \\ \boldsymbol{c}_{qu} & \boldsymbol{c}_{qq} \end{bmatrix} \cdot \begin{Bmatrix} \boldsymbol{u} \\ \boldsymbol{q} \end{Bmatrix} = \begin{Bmatrix} \boldsymbol{f}_u \\ \boldsymbol{f}_q \end{Bmatrix} \quad (1)$$

In (1), $\boldsymbol{u}$ are the local structural and aerodynamic DOFs. In the case of a rotor blade, $\boldsymbol{u}$ will include the local bending (flapwise and edgewise), tension and torsion DOFs plus the additional circulation states introduced by the ONERA aerodynamic model [12]. The vector $\boldsymbol{q}$ contains all the rigid body translations and rotations, determining the origin and orientation

of the local to the body co-ordinate system with respect to the inertial frame. In particular, for the blade, vector $\boldsymbol{q}$ can both include large rotations and translations (e.g. azimuth rotation, pitching motion, yaw of the nacelle) but also structural deflections of preceding bodies (e.g. bending displacements and rotations at the tower top and hub centre attachment points). In the context of a multi-body approach these are all treated uniformly as rigid body motions.

Given the above definitions of $\boldsymbol{u}$ and $\boldsymbol{q}$, it follows that the off-diagonal elements in the mass, damping and stiffness matrices in (1), designated with the subscript 'uq', correspond to the coupling terms resulting from the relative motion of the local system with respect to the global inertial frame while those indicated by 'qu' correspond to the kinematic or structural dependency of the $\boldsymbol{q}$ DOFs on the local $\boldsymbol{u}$ DOFs.

In open loop operation, fixed value conditions are appointed to the $\boldsymbol{q}$ DOFs, associated with specific control output variables. For example, for a pitch regulated–variable speed wind turbine it is assumed that the generator speed and the pitch angle of the blades are time-invariant. The fixed values imposed to these DOFs are representative of the average operation conditions for a specific wind speed. Such an assumption will of course constrain the loads associated with the specific kinematic DOFs, i.e. the torque of the generator and the pitching torque at the root of the blades.

To obtain the linearized system of equations (1) the non-linear servo-aeroelastic equations of motion are linearized with respect to a reference state.

The linearized system (1) is reformulated into a first order system:

$$\dot{\boldsymbol{x}} = \boldsymbol{A}(\boldsymbol{x}_0, \dot{\boldsymbol{x}}_0) \cdot \boldsymbol{x} + \boldsymbol{B} \qquad (2)$$

In (2) $\boldsymbol{x}_0$ denotes the reference state and $\boldsymbol{x}$ are perturbations of the state variables about this reference state. The reference state can either be periodic or steady depending on the type of the dynamic system considered and its excitation. In the present work where the isolated parked blade problem is dealt with, the reference state is steady and it is obtained by solving the static problem stemming from (1) when deflection velocities and accelerations are set to zero. The eigenvalues of the constant coefficient matrix $\boldsymbol{A}$ provide the natural frequencies and damping characteristics of (2). On the contrary, when the stability of the blade is examined during operation, the reference state is a periodic equilibrium solution defined by integrating the non-linear set of equations in time until a periodic response (with respect to the rotor speed) is reached. In this case a multi-blade transformation of the rotating DOFs is introduced to eliminate the periodic coefficients arising and treat the linear system with reference to the non-rotating frame.

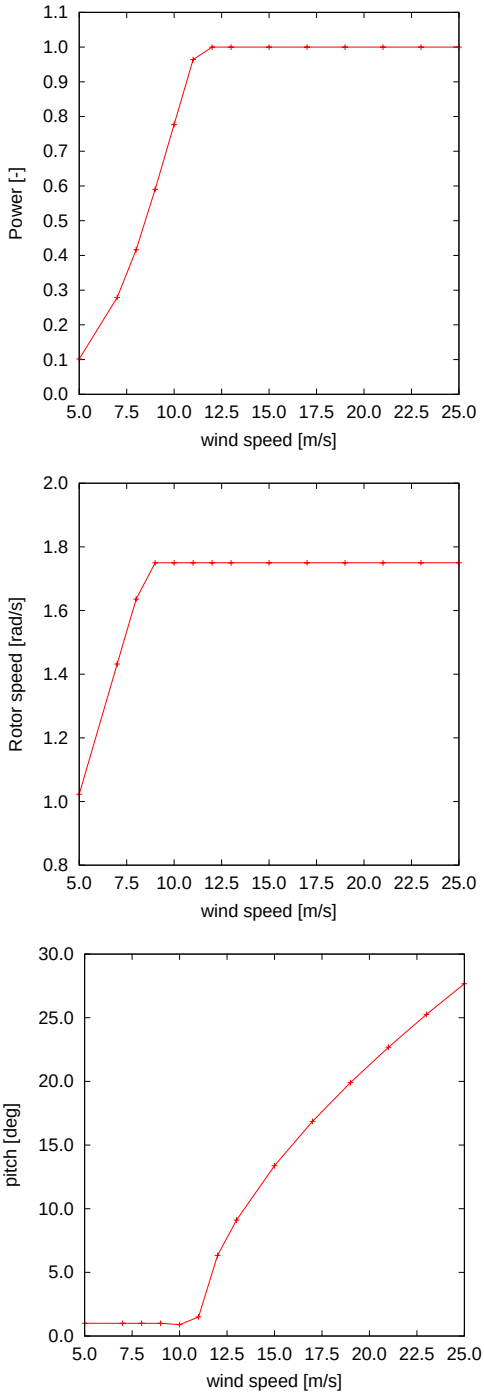

Figure 1: Power curve and operational characteristics of the reference rotor.

Mode Description	Natural frequency [Hz]	
	0 rpm	16.7 rpm
1st flap	1.17	1.24
1st lag	1.55	1.56
2nd flap	2.95	3.04
2nd lag	4.31	4.35
3rd flap	5.95	6.03
3rd lag	9.41	9.46

Table 1: Natural frequencies in vacuum.

3 The reference blade

The analysis presented in this paper concerns a reference blade (around 40 m) designed within the context of Work Package 1B1 of the UpWind project. In the analysis, the blade is assumed infinitely stiff in torsion, and this is the reason why no information for the torsional structural modes of the blade is presented hereafter. Also, structural damping is not taken into account.

In Table 1 the natural frequencies of the reference blade in vacuum for the rotor speeds of 0 rpm and 16.7 rpm (nominal speed) are included for the first six modes (three flapwise and three lagwise). It is noted that the first flapwise and lead-lag eigen-frequencies are quite close to each other. The former is found in the vicinity of 4 P (slightly higher), while the latter is near 5.5 P. This design approach slightly deviates from the common design practice, which places first flapwise frequency near 4 P (or slightly lower) and the first lead-lag frequency near 6.5–7 P (or slightly lower).

The operational characteristics of the reference rotor (rotational speed and pitch angle) are presented in Figure 1, along with its power curve. An isolated rotor stability analysis has been performed, in which it is assumed that the wind turbine operates in open loop. This means that at each wind speed, the rotational speed of the rotor and the blade pitch obtain constant values that correspond to the average conditions presented in Figure 1. In these computations structural damping has not been taken into account. Whilst this analysis is not strictly within the frame of the present work, it provides the necessary evidence that the blade is stable in normal operation.

The distribution of the aero-elastic frequencies are presented in Figure 2 for the first four structural modes (two flapwise and two lagwise). The first flapwise and lead-lag eigenfrequencies are quite close to each other, as already noted in the vacuum frequencies. The effect of the flap lead-lag frequency coincidence on the stability of a rotor has been extensively investigated in [16]. There it was shown that as a consequence of the

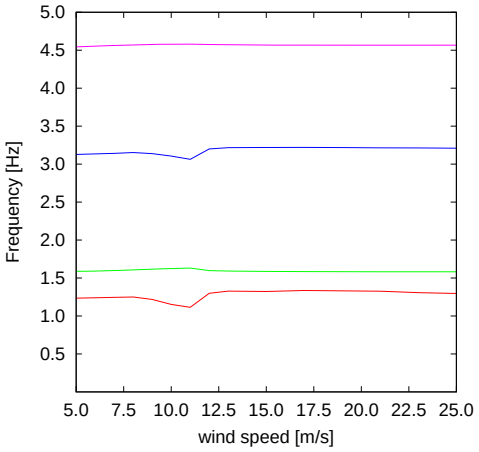

Figure 2: Aeroelastic frequencies of the blade.

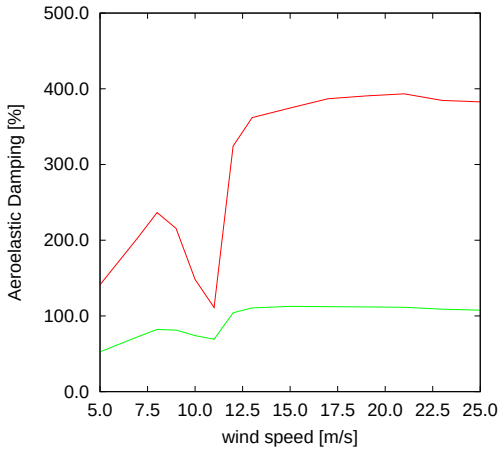

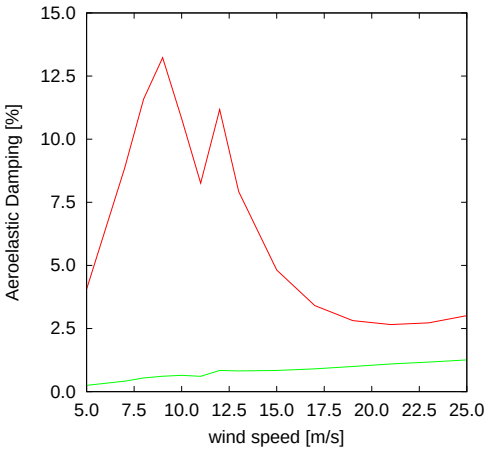

Figure 3: Aeroelastic damping of the first (red curve) and second (green curve) flap (upper) and lead-lag (lower) modes.

proximity of the two frequencies high damping values are expected for the, usually low damped, first lead-lag mode.

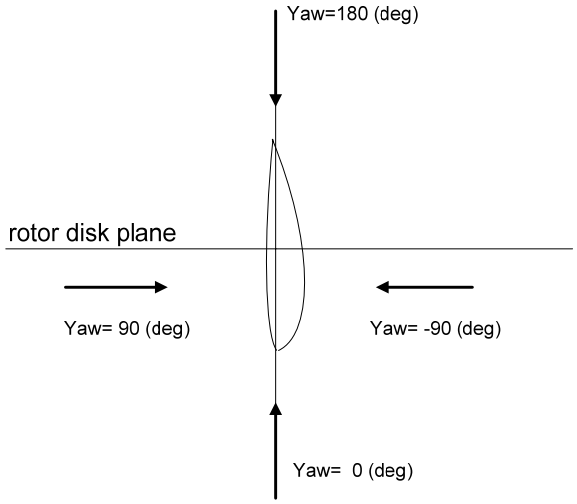

Figure 4: Definition of the yaw angle.

The aerodynamic damping is plotted in Figure 3 in terms of the logarithmic decrement of the first four structural modes (two flap and two lead-lag). It is important to note that even by neglecting structural damping in this analysis, the damping values that arise are positive for all modes. In particular flapwise modes are highly damped and lead-lag modes are low damped, as expected.

As a result of the proximity of the first flap and lead-lag modes, high damping values of the first lead-lag mode are obtained in the vicinity of the rated speed. The slight dip on the damping of all modes near the rated speed is connected to the stalled operation of the rotor just before pitch starts to vary. Then, as the pitch angle increases the damping also starts to increase. This is especially true in the case of the flap modes. As regards the first lead lag mode the damping drops considerably at high wind speeds within the variable pitch region.

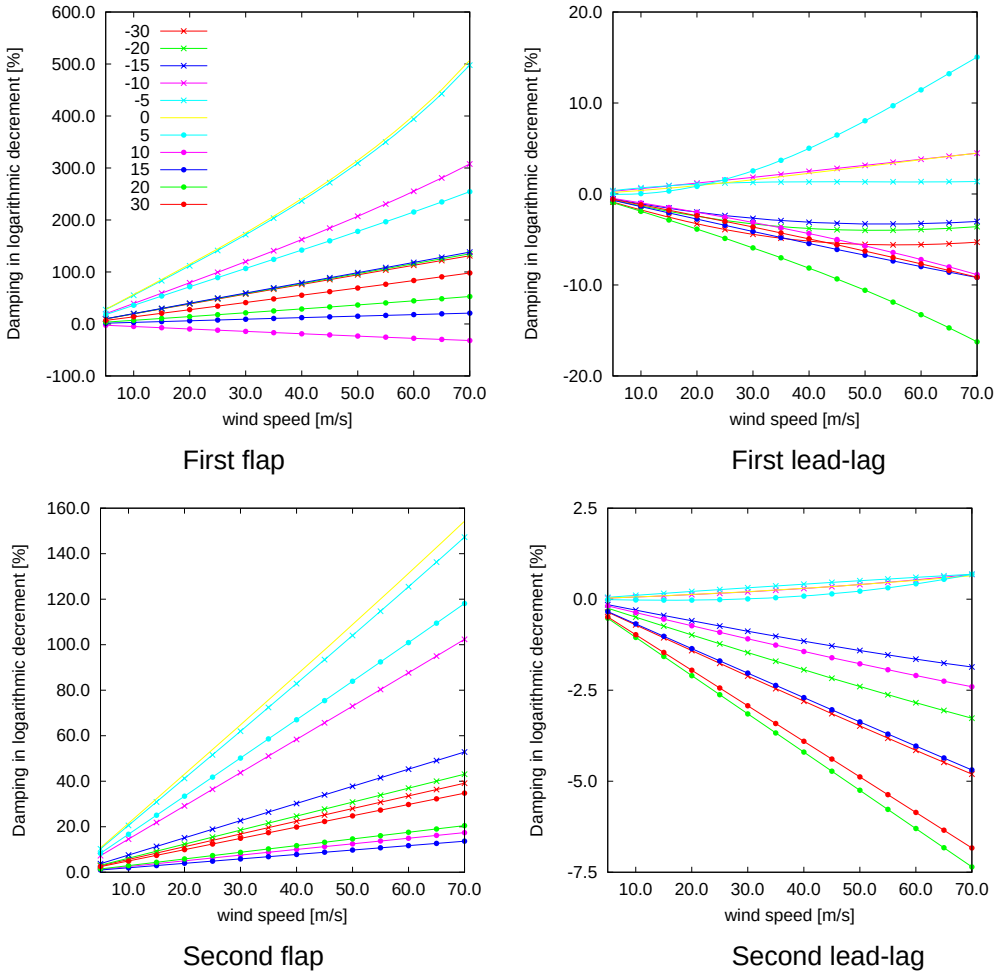

Figure 5: Aeroelastic damping of the first four structural modes for different yaw angles using quasi-steady modelling.

4 Results and discussion

4.1 Isolated rotor analysis using quasi-steady aerodynamics

The results of the analysis of the parked blades are presented in this section. As regards the sign of the yaw error the standard definition illustrated in Figure 4 is followed. According to the figure, when the yaw error is 90^0, the incoming flow is perpendicular to the blade and the blade encounters large positive angles of attack while when -90^0 is again perpendicular but the angles of attack are negative. So 0^0 yaw angle corresponds to the case that the chordwise direction of the blade is aligned to the incoming wind flow. On the other hand 180^0 and -180^0 corresponds to the case that the flow comes backwards.

The damping characteristics of the first four modes of the parked blade versus wind speed (ranging from 5–70 m/s) and for various yaw angles (ranging from -30^0 to 30^0) are presented in Figure 5. In Figure 6 the dependency of the modal damping on the yaw error is shown for the same modes and for four different speeds (25, 35, 50 and 70 m/s). In these plots the yaw error varies from -180^0 to 180^0, which means that all possible directions of the incoming flow are considered.

In this first set of computations stability analysis is performed using steady-state aerodynamics. In all computations zero structural damping has been assumed, so the damping values shown in the figures represent solely aerodynamic damping of the blade. For the pitch regulated wind turbine considered it is assumed that the blade, when parked, is in feather position (90^0 pitched, see Figure 4).

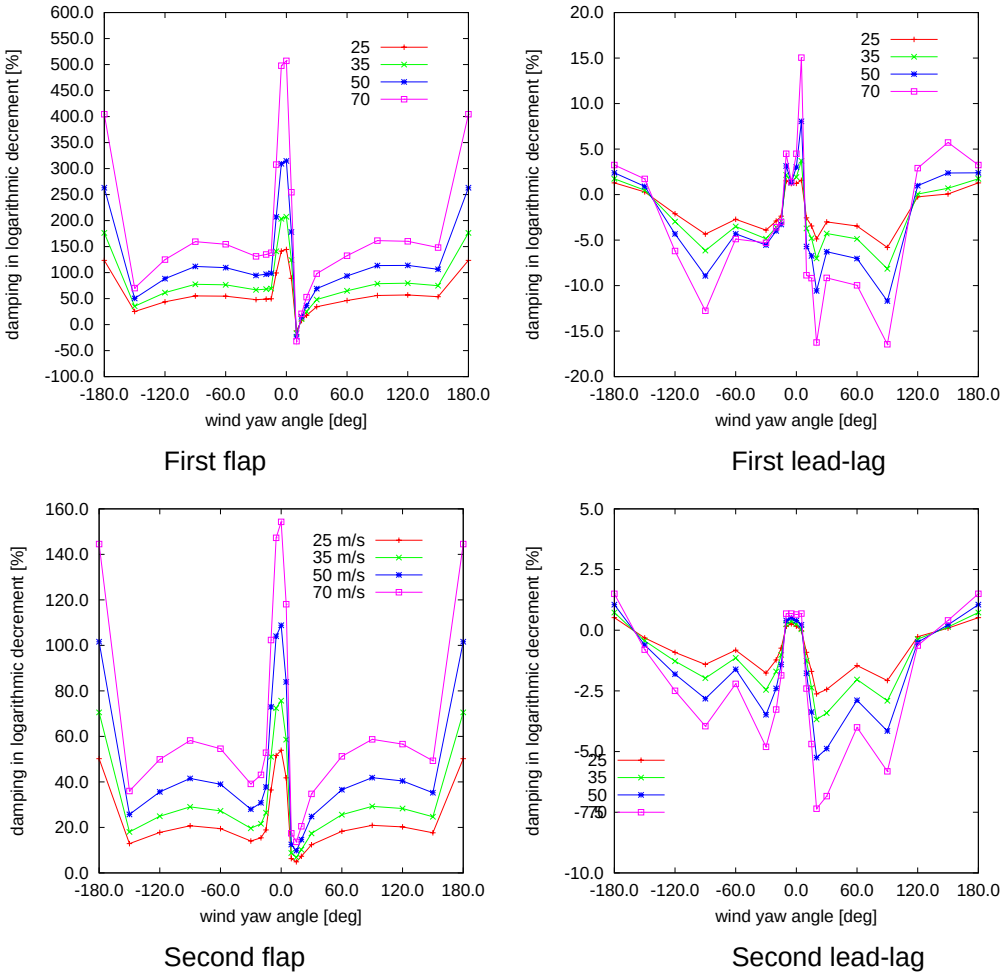

Figure 6: Aeroelastic damping of the first four structural modes for different wind speed values using quasi-steady modelling.

From the above results the following general conclusions are drawn:

• The highest aerodynamic damping is produced at small (positive or negative) yaw angles and for backward flow.
• The lowest aerodynamic damping is showed at angles of attack around C_{Lmax} and $\pm 90^0$.
• The first flap mode becomes negatively damped at 10^0 yaw angle as a result of the blade operation in the "near" post stall region. However, the appearance of negative damping values is local and it is only limited to a narrow incidence band.
• Edgewise vibrations (if any) would increase with the wind speed. This is true at all yaw error angles but the low and moderate negative ones. In the latter case, the damping tends to a constant negative value or even slightly increases at high wind speeds.

4.2 Isolated rotor analysis using unsteady aerodynamics

The damping results obtained by the application of the unsteady aerodynamics model ONERA are presented in Figure 7. Unsteady aerodynamic computations are performed for the range of yaw angles of $[-15^0, 30^0]$. This is because beyond that range the results of the ONERA model are no longer trustworthy. In Figure 7, the unsteady aerodynamic predictions are compared against the steady state results for the first flap and first lead-lag modes and for four wind speeds (25, 35, 50 and 70 m/s). From this comparison it is concluded that in the use of unsteady aerodynamics:

• the damping of the first flap mode remains positive at all yaw angles examined, as long as the wind speed does not exceed 25 m/s. At higher wind speeds, negative damping values of the first flap mode are obtained with some delay as compared to the steady state predictions. Minimum damping values are obtained at the yaw angle of 20^0.
• at low yaw angles, the damping of the first flap mode is lower than the one obtained with steady-state aerodynamics. As the wind speed increases the difference between steady and unsteady predictions becomes smaller and smaller. The lower damping values obtained at low wind speeds is explained by the Theodorsen effect on the unsteady C_L hysteresis loops. Of course as the wind speed increases damping is dominated by the wind velocity rather than the C_L dependency on the local flow angle of attack.
• negative damping values of the first lead-lag mode predicted by the ONERA model are higher than those predicted using steady state aerodynamics.

The above predictions, although they clearly provide an indication of the flow conditions under which instabilities are more likely to occur, are still subjected to uncertainties especially when massively separated flows are dealt with. So they definitely need to be verified through computations using even more advanced aerodynamic models. Also, additional parameters that need to be addressed are the non linearity of the flow and its effect on the damping predictions, as well as the fact that, in most cases, parked rotors are not standing still but they idle. It is expected that both parameters would have a positive effect on stability that needs to be accounted for in future developments.

In order to moderate these uncertainties, at a later stage, a free-wake aerodynamic model will be employed. It is based on vortex particle approximations of the wake, where free vorticity is released along the trailing edge and tip of the blade. In cases of massive separation, the release of vortex particles is extended along the leading edge resulting in a "double wake" [17]. The two vortex sheets interact with each other and through their role up they form a separation bubble that extends over the suction side of the blade. Simulations using this kind of modelling will be performed in the time domain and stability analysis will be carried out on the resulting time series.

5 Conclusions

The aeroelastic stability of a parked wind turbine rotor is addressed in this paper in the context of a linear eigenvalue analysis assuming steady-state aerodynamics (unsteady vortex shedding is not taken into account) for yaw angles ranging from -180^0 to 180^0 or unsteady aerodynamic modelling for relatively low yaw angles, for wind speeds up to the survival speed of 70 m/s. It provides a first estimate of the angle of attack regimes for which stall induced vibrations might become more pronounced. These uncertainties will be addressed at a later stage, using a free-wake aerodynamic modelling.

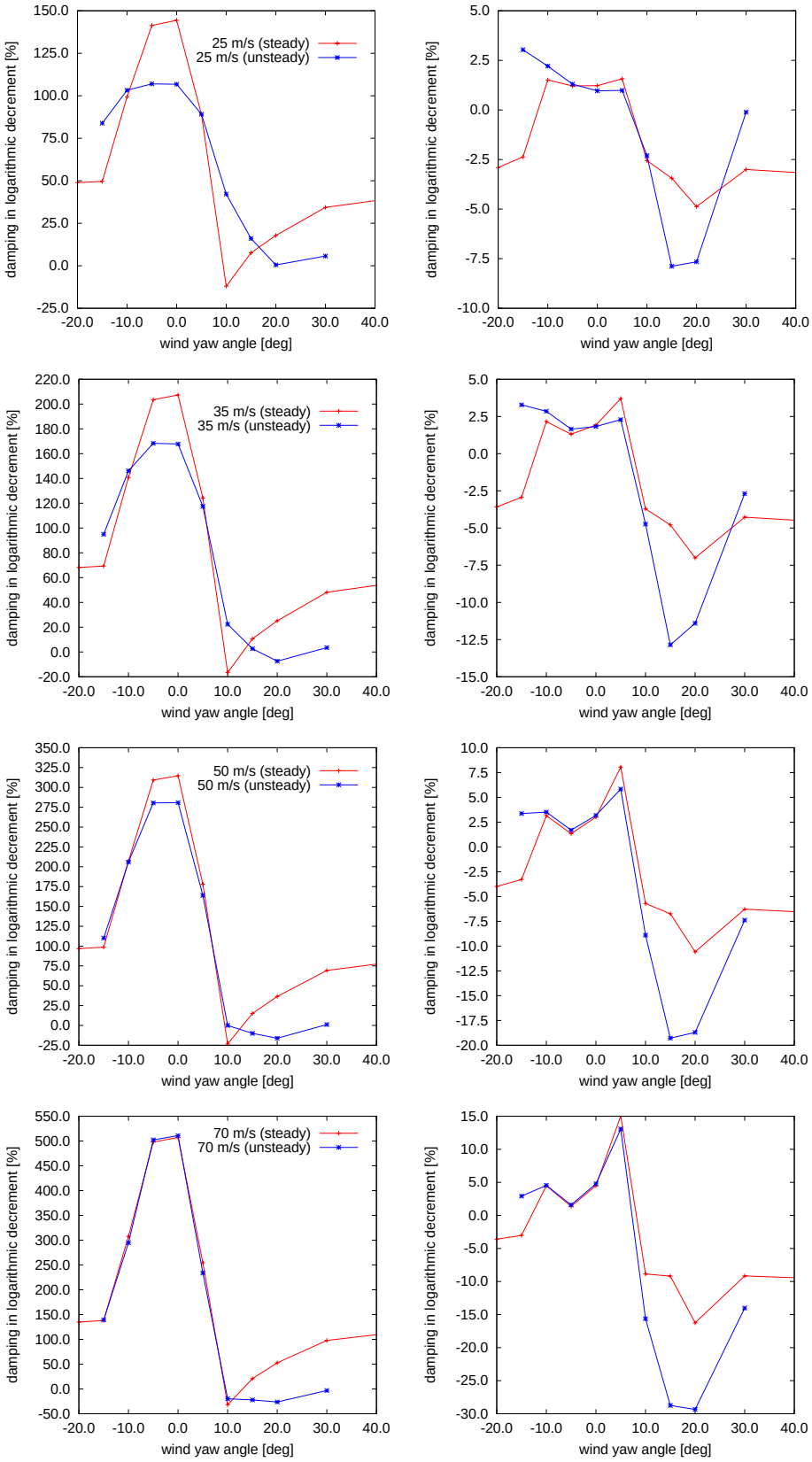

Figure 7: Aeroelastic damping of the first flap (left) and first lead-lag (right) modes for different wind speeds using unsteady aerodynamic (ONERA) modelling (comparison with steady-state predictions).

From the analysis with the steady-state aerodynamic model it is concluded that the highest aerodynamic damping occurs at small (positive or negative) yaw angles and for backward flow. The lowest aerodynamic damping occurs at yaw angles of 20^0 (angles of attack slightly beyond C_{Lmax} angles) and $\pm 90^0$. The, generally highly damped, first flap mode becomes negatively damped at 10^0 yaw angle as a result of the blade operating in the "near" post stall region. However, the appearance of negative damping values is local and it is only limited to a narrow incidence band.

In the case of the unsteady aerodynamic modelling the damping of the first flap mode does not become negative at moderate positive yaw angles (around 10^0) as long as the wind speed is lower than 25 m/s. At higher wind speeds negative aerodynamic damping values of the first flap mode are obtained with some delay at higher yaw angles (around 20^0). The negative damping values of the first lead-lag mode predicted by the unsteady model are higher than those predicted using steady state aerodynamics.

The above predictions, although they clearly provide an indication of the flow conditions under which instabilities are more likely to occur, they are still subjected to uncertainties especially when massively separated flows are dealt with.

Acknowledgements

This work was supported by the European Commission under contract SES6, 019945.

References

[1] Petersen, J.T., Madsen, H.A., Bjørck, A., Enevoldsen, P., Øye, S., Ganander, H., Winkelaar, D., "Prediction of Dynamic Loads and Induced Vibrations in Stall," Risø-R-1045(EN), Risø National Laboratory, Roskilde, 1998

[2] Hansen, M.H., "Improved Modal Dynamics of Wind Turbines to Avoid Stall Induced Vibrations," Wind Energy, 2003, 6, 179–195

[3] Chaviaropoulos, P. K., "Flap/Lead–lag Aero-elastic Stability of Wind Turbine Blades," Wind Energy, 2001, 4, 183–200.

[4] Markou, H.,Hansen, M.H., Buhl, T., Engelen, T. van, Politis, E.S., Riziotis,V.A., Poulsen, N.K., Larsen, A.J., Mogensen, T.S., Holierhoek, J.G., "Aeroelastic Stability and Control of Large Wind Turbines – Main Results," Proceedings of the 2007 European Wind Energy Conference & Exhibition, Milan.

[5] Rasmussen, F., Petersen, J.T., Madsen, H.A., "Dynamic Stall and Aerodynamic Damping," ASME Journal of Solar Energy Engineering 1999, 121, 150–155.

[6] Hansen M.H., Gaunna M., Madsen H.A., "A Beddoes-Leishman Type Dynamic Stall Model in State-space and Indicial Formulations," Risø-R-1354(EN), Risø National Laboratory, Roskilde, 2003.

[7] Ekaterinaris J.A. and Platzer, M.F., "Computational Prediction of Airfoil Dynamic Stall", Prog. Aerospace Sci., 1998, vol. 33, pp. 759–846.

[8] Chaviaropoulos P.K., Nikolaou I.G., Aggelis K.A., Sørensen N.N., Johansen J., Hansen M.O.L., Mac Gaunaa, Hambraus T., von Geyr H.Frhr., Hirsch Ch., Kang Shun, Voutsinas S. G., Tzabiras G., Perivolaris Y. and Dyrmose S.Z., "Viscous and Aeroelastic Effects on Wind Turbine Blades. The VISCEL project. Part I: 3D Navier-Stokes Rotor Simulations," Wind Energy, 2003, 6, 365–385.

[9] Chaviaropoulos P.K., Sørensen N.N Hansen M.O.L., Nikolaou I.G., Aggelis K.A., Johansen J., Mac Gaunaa, Hambraus T., von Geyr H.Frhr., Hirsch Ch., Kang Shun, Voutsinas S. G., Tzabiras G., Perivolaris Y. and Dyrmose S.Z., "Viscous and Aeroelastic Effects on Wind Turbine Blades. The VISCEL Project. Part II: Aeroelastic Stability Investigations," Wind Energy, 2003, 6, 387–403.

[10] Hansen, M.H., "Aeroelastic Instability Problems for Wind Turbines," Wind Energy 2007, 10, 551–557.

[11] Hansen, M.O.L., Sørensen, J.N., Voutsinas, S., Sørensen, N., Madsen, H.A., "State of the Art in Wind Turbine Aerodynamics and Aeroelasticity," Progress in Aerospace Sciences, 2006, 42 285–330.

[12] Riziotis, V. A., Voutsinas, S. G., Politis, E. S. and Chaviaropoulos, P. K., "Aeroelastic Stability of Wind Turbines: The Problem, the Methods and the Issues," Wind Energy, 2004, 7, 373–392.

[13] Riziotis, V. A., Voutsinas, S. G., Politis, E. S. and Chaviaropoulos, P. K., "Stability Analysis of Pitch-regulated, Variable Speed Wind Turbines in Closed Loop Operation

Using a Linear Eigenvalue Approach," Wind Energy, 2008, 11, 517–535.

[14] Riziotis, V.A. and Voutsinas, S.G., "GAST: A General Aerodynamic and Structural Prediction Tool for Wind Turbines," Proceedings of the 1997 European Wind Energy Conference & Exhibition, Dublin, Ireland.

[15] Petot, D., "Differential Equation Modelling of Dynamic Stall," Recherché Aerospatiale, 1989, 5, 59–72.

[16] Riziotis, V.A., Voutsinas, S.G., Politis, E.S., Chaviaropoulos, P.K. (2008) "Assessment of Passive Instability Suppression Means on Pitch Regulated Wind Turbines," Wind Energy, 2008, 11, pp 171–192.

[17] Riziotis,V.A. and Voutsinas, S.G. (1997) "Dynamic Stall on Wind Turbine Rotors: Comparative Evaluation Study of Different Models," Proceedings of the 1997 European Wind Energy Conference & Exhibition, Dublin, Ireland.